JCI The Journal of Clinical Investigation

Proteasome function is required for platelet production

Dallas S. Shi, … , Dean Y. Li, Andrew S. Weyrich

J Clin Invest. 2014;124(9):3757-3766. https://doi.org/10.1172/JCI75247.

Research Article **Hematology**

The proteasome inhibiter bortezomib has been successfully used to treat patients with relapsed multiple myeloma; however, many of these patients become thrombocytopenic, and it is not clear how the proteasome influences platelet production. Here we determined that pharmacologic inhibition of proteasome activity blocks proplatelet formation in human and mouse megakaryocytes. We also found that megakaryocytes isolated from mice deficient for PSMC1, an essential subunit of the 26S proteasome, fail to produce proplatelets. Consistent with decreased proplatelet formation, mice lacking PSMC1 in platelets (*Psmc1*$^{fl/fl}$ *Pf4-Cre* mice) exhibited severe thrombocytopenia and died shortly after birth. The failure to produce proplatelets in proteasome-inhibited megakaryocytes was due to upregulation and hyperactivation of the small GTPase, RhoA, rather than NF-κB, as has been previously suggested. Inhibition of RhoA or its downstream target, Rho-associated protein kinase (ROCK), restored megakaryocyte proplatelet formation in the setting of proteasome inhibition in vitro. Similarly, fasudil, a ROCK inhibitor used clinically to treat cerebral vasospasm, restored platelet counts in adult mice that were made thrombocytopenic by tamoxifen-induced suppression of proteasome activity in megakaryocytes and platelets (*Psmc1*$^{fl/fl}$ *Pdgf-Cre-ER* mice). These results indicate that proteasome function is critical for thrombopoiesis, and suggest inhibition of RhoA signaling as a potential strategy to treat thrombocytopenia in bortezomib-treated multiple myeloma patients.

Proteasome function is required for platelet production

Dallas S. Shi,[1,2,3] Matthew C.P. Smith,[1,3,4] Robert A. Campbell,[1] Patrick W. Zimmerman,[1] Zechariah B. Franks,[1] Bjorn F. Kraemer,[1] Kellie R. Machlus,[5,6] Jing Ling,[1] Patrick Kamba,[1] Hansjörg Schwertz,[1,7] Jesse W. Rowley,[1,3] Rodney R. Miles,[8] Zhi-Jian Liu,[6,9] Martha Sola-Visner,[6,9] Joseph E. Italiano Jr.,[5,6,10] Hilary Christensen,[11] Walter H.A. Kahr,[11,12] Dean Y. Li,[1,2,3,4,13] and Andrew S. Weyrich[1,3]

[1]The Molecular Medicine Program, [2]Department of Human Genetics, [3]Department of Internal Medicine, and [4]Department of Oncological Sciences, University of Utah, Salt Lake City, Utah, USA. [5]Division of Hematology, Department of Medicine, Brigham and Women's Hospital, Boston, Massachusetts, USA. [6]Harvard Medical School, Boston, Massachusetts, USA. [7]Department of Immunology and Transfusion Medicine, Ernst-Moritz-Arndt University of Greifswald, Greifswald, Germany. [8]Department of Pathology, University of Utah, Salt Lake City, Utah, USA. [9]Division of Newborn Medicine and [10]Vascular Biology Program, Department of Surgery, Children's Hospital, Boston, Massachusetts, USA. [11]Division of Haematology/Oncology, Program in Cell Biology, The Hospital for Sick Children, Toronto, Ontario, Canada. [12]Departments of Paediatrics and Biochemistry, University of Toronto, Toronto, Ontario, Canada. [13]Key Laboratory for Human Disease Gene Study of Sichuan Province, Institute of Laboratory Medicine, Sichuan Academy of Medical Sciences and Sichuan Provincial People's Hospital, Chengdu, Sichuan, People's Republic of China.

The proteasome inhibiter bortezomib has been successfully used to treat patients with relapsed multiple myeloma; however, many of these patients become thrombocytopenic, and it is not clear how the proteasome influences platelet production. Here we determined that pharmacologic inhibition of proteasome activity blocks proplatelet formation in human and mouse megakaryocytes. We also found that megakaryocytes isolated from mice deficient for PSMC1, an essential subunit of the 26S proteasome, fail to produce proplatelets. Consistent with decreased proplatelet formation, mice lacking PSMC1 in platelets (*Psmc1*$^{fl/fl}$ *Pf4-Cre* mice) exhibited severe thrombocytopenia and died shortly after birth. The failure to produce proplatelets in proteasome-inhibited megakaryocytes was due to upregulation and hyperactivation of the small GTPase, RhoA, rather than NF-κB, as has been previously suggested. Inhibition of RhoA or its downstream target, Rho-associated protein kinase (ROCK), restored megakaryocyte proplatelet formation in the setting of proteasome inhibition in vitro. Similarly, fasudil, a ROCK inhibitor used clinically to treat cerebral vasospasm, restored platelet counts in adult mice that were made thrombocytopenic by tamoxifen-induced suppression of proteasome activity in megakaryocytes and platelets (*Psmc1*$^{fl/fl}$ *Pdgf-Cre-ER* mice). These results indicate that proteasome function is critical for thrombopoiesis, and suggest inhibition of RhoA signaling as a potential strategy to treat thrombocytopenia in bortezomib-treated multiple myeloma patients.

Introduction

Thrombocytopenia (low platelet count) is observed in numerous diseases and can be life threatening due to bleeding complications. Bortezomib, a reversible chemotherapeutic inhibitor used to treat patients with relapsed multiple myeloma, often induces thrombocytopenia within a few days of therapy initiation (1–3). Bortezomib-induced thrombocytopenia is dose-limiting, and if severe, bortezomib is withheld (2, 3). Although the mechanisms by which bortezomib induces thrombocytopenia is not clear, its primary mode of action is inhibition of the proteasome. The clinical observation that platelet counts rise above pretherapy levels upon cessation of bortezomib treatment suggests that bortezomib affects thrombopoiesis (1, 3).

Like other cells, megakaryocytes and anucleate platelets possess proteasome activity (4, 5). While the specific functions of the proteasome in platelet precursors (e.g., megakaryocytes) is relatively unknown (6), there is evidence that bortezomib alters the function of platelets (7–11). It has also been hypothesized, but not proven, that bortezomib inhibits megakaryocyte development via nuclear factor κB (NF-κB) (12). The aim of the present work was to precisely define the roles of the proteasome in thrombopoiesis and, in doing so, determine whether bortezomib-induced thrombocytopenia can be reversed. Using a combination of pharmacologic and genetic tools, we showed that inhibition of proteasome activity in megakaryocytes blocks proplatelet formation. In addition, conditional deletion of proteasome activity in mouse megakaryocytes led to severe thrombocytopenia and postnatal death. Decreased thrombopoiesis in proteasome-inhibited mice was caused by accumulation and increased activity of RhoA, and inhibitors of the RhoA signaling pathway restored platelet production. These findings demonstrated that the megakaryocyte proteasome controls the final stages of platelet production and also provided a potential option for restoring platelet counts in thrombocytopenic patients treated with bortezomib.

Results

Pharmacologic inhibition of the proteasome blocks platelet production. Due to its thrombocytopenic side effects, bortezomib is typically administered as a bolus twice weekly for 2 weeks (days 1, 4, 8, and 11), followed by a 10-day rest period (3). To ascertain the immediate effects of this inhibitor on platelets, mice were administered a clinically relevant dose (2 mg/kg body weight) of bortezomib, and platelet counts and proteasome activity were measured. Consistent with its well-known effect on platelet counts in patients, bortezomib induced a mild thrombocytopenia within 24 hours of

Authorship note: Dallas S. Shi and Matthew C.P. Smith contributed equally to this work.
Conflict of interest: The authors have declared that no conflict of interest exists.
Submitted: January 17, 2014; **Accepted:** June 5, 2014.
Reference information: *J Clin Invest*. 2014;124(9):3757–3766. doi:10.1172/JCI75247.

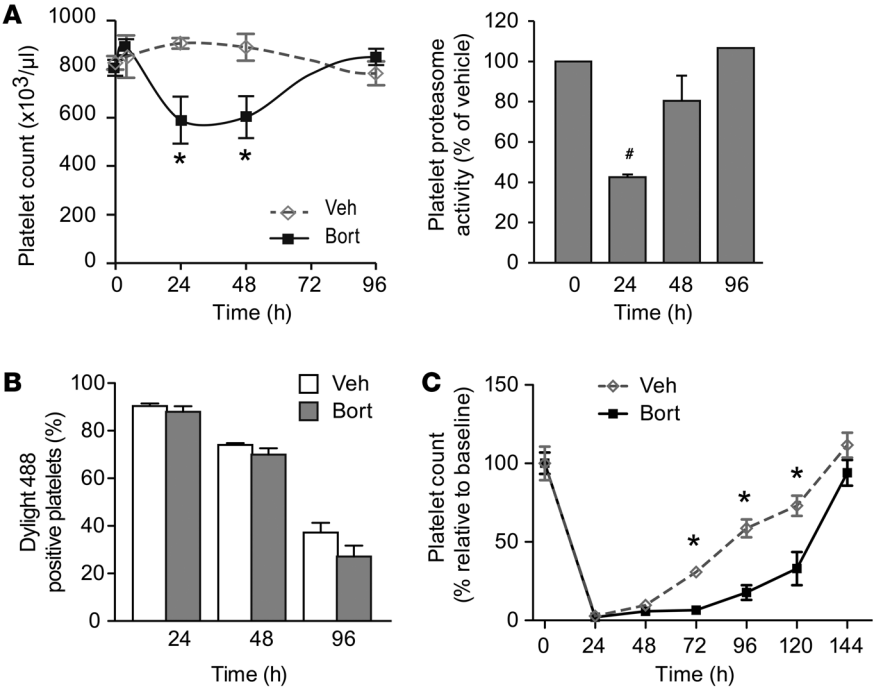

Figure 1. Pharmacologic inhibition of the proteasome induces thrombocytopenia in mice by decreasing platelet production. (**A**) Mice were treated with a bolus of bortezomib (Bort) or vehicle (Veh), and platelet counts and platelet proteasome activity were measured at the indicated times. Data are mean ± SEM of 6 experiments. (**B**) Mouse platelets were labeled in vivo with Dylight 488, as described in Methods. In parallel, the mice were treated with a bolus of bortezomib or vehicle, and the percentage of labeled platelets was determined at 24, 48, and 96 hours after treatment. Data are mean ± SEM of 6 independent experiments. (**C**) Mouse platelets were depleted in the presence of bortezomib or its vehicle, as described in Methods. The percentage of platelets relative to baseline control (0 hours) is shown. Data are mean ± SEM of 5 independent experiments. Note that **A**–**C** are derived from separate experiments. $^{*}P < 0.05$ vs. vehicle; $^{\#}P < 0.05$ vs. 0 hours.

treatment (Figure 1A). The thrombocytopenia was transient and temporally correlated with inhibition of proteasome activity in circulating platelets (Figure 1A).

To assess whether bortezomib-induced thrombocytopenia was due to accelerated clearance, we injected Dylight 488 conjugated to GPIBβ into the bloodstream to track the lifespan of platelets in vivo in the presence of bortezomib or its vehicle. As expected, the number of labeled platelets decreased over 96 hours as platelets were cleared from the circulation (13). However, the number of labeled platelets was similar between bortezomib and vehicle treatment groups at every time point tested (Figure 1B). This suggested that bortezomib did not induce platelet activation in the bloodstream, which would facilitate platelet clearance. Consistent with this notion, we found that bortezomib did not directly induce activation of integrin $\alpha_{IIb}\beta_3$ (Supplemental Figure 1; supplemental material available online with this article; doi:10.1172/JCI75247DS1), nor did it alter agonist-induced activation of integrin $\alpha_{IIb}\beta_3$ or surface expression of P-selectin in mouse platelets (Supplemental Figures 1 and 2). Similarly, bortezomib did not influence PAC-1 binding to human platelets in the presence or absence of agonist stimulation (Supplemental Figure 3 and data not shown).

Since acute administration of bortezomib did not shorten the lifespan of circulating platelets, we hypothesized that the bortezomib-induced thrombocytopenia was due to a decrease in platelet production. To test this, we depleted platelets with an antibody against GPIBα and then treated mice with bortezomib or its vehicle to determine whether bortezomib prevented platelet counts from rebounding. Platelet counts rebounded at a slower pace with bortezomib treatment than with the vehicle control (Figure 1C).

The data in Figure 1 suggested that bortezomib-induced thrombocytopenia was due to a defect in the formation of platelets from megakaryocytes. To examine this further, we determined whether inhibition of the proteasome with bortezomib blocked proplatelet formation in murine megakaryocytes. Bortezomib significantly decreased proplatelet formation in fetal liver–derived megakaryocytes (Figure 2A). Similar responses were observed in human megakaryocytes, and removal of bortezomib from the incubation media restored proplatelet formation (Figure 2B and data not shown). To confirm that this effect was specific to proteasome inhibition, megakaryocytes were treated with MG132 or lactacystin. Both proteasome inhibitors phenocopied the effects of bortezomib (Supplemental Figure 4 and data not shown). The inability to form proplatelets was accompanied by a notable increase in cell spreading on immobilized fibrinogen (Figure 2B), which indicates that the proteasome regulates key cytoskeletal proteins in megakaryocytes.

Phenotypic consequences of proteasome inhibition are independent of NF-κB and integrin α_{IIb}. Bortezomib's antitumor activity in multiple myeloma has been attributed to inhibition of NF-κB in plasma cells (14). Therefore, others have speculated that proteasome inhibitors may induce thrombocytopenia via the NF-κB signaling pathway (12). To test this hypothesis, we first treated megakaryocytes with bortezomib and examined the expression of nuclear factor of κ light polypeptide gene enhancer in B cells inhibitor, α (IκBα), which sequesters NF-κB in the cytoplasm until it is phosphorylated, ubiquitinated, and degraded (15). As expected, bortezomib increased the expression of IκBα in megakaryocytes (Figure 3A), which demonstrated that inhibition of the proteasome blocks the NF-κB signaling pathway. We also found that inhibition of IκB kinase with SC-514, which induces IκBα phosphorylation, increased IκBα protein levels in megakaryocytes (Figure 3A). However, unlike bortezomib, SC-514 did not halt proplatelet production (Figure 3B).

In addition to regulating NF-κB activity, Mitchell and colleagues previously demonstrated that the proteasome is capable of degrading pro–integrin α_{IIb} (5). Based on this published work, and our present finding that inhibition of the proteasome decreased

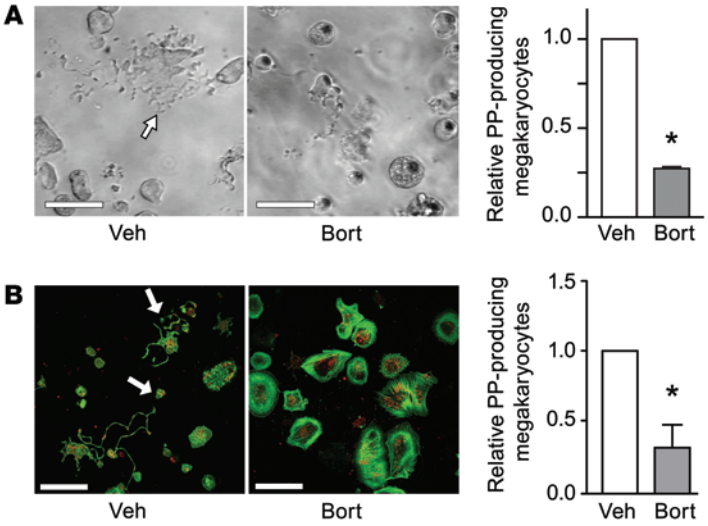

Figure 2. Pharmacologic inhibition of the proteasome blocks proplatelet formation in murine and human megakaryocytes. Mouse fetal liver–derived megakaryocytes (**A**) and human megakaryocytes (**B**) were pretreated with vehicle or bortezomib, and megakaryocytes producing proplatelets (PP) were examined. Shown are (**A**) representative transmission images and (**B**) representative confocal images with wheat germ agglutinin (WGA; red) and phalloidin (green) staining. Arrows denote proplatelet extensions. Also shown for each is the number of proplatelet-producing megakaryocytes relative to vehicle control. Data are mean ± SEM of 3 independent experiments. *$P < 0.05$ vs. vehicle. Scale bars: 100 μm (**A**); 50 μm (**B**).

the formation of proplatelets when megakaryocytes adhere to fibrinogen, we sought to determine whether bortezomib regulated the activity of integrin $\alpha_{IIb}\beta_3$ in megakaryocytes. Bortezomib did not alter the expression of mature integrin α_{IIb} protein, nor did it increase binding of soluble fibrinogen or PAC-1 to human megakaryocytes (Supplemental Figure 5 and data not shown). Bortezomib also had no effect on adherence of human megakaryocytes to fibrinogen (Supplemental Figure 6). Together, these data indicate that bortezomib does not directly block proplatelet formation through NF-κB– or integrin $\alpha_{IIb}\beta_3$–dependent mechanisms.

Phenotypic consequences of proteasome inhibition require RhoA. The changes in actin polymerization observed in megakaryocytes treated with proteasome inhibitors were reminiscent of cytoskeletal changes in endothelial cells that rely on the small GTPase RhoA (16). Indeed, we found that bortezomib increased total RhoA protein expression (Figure 4A). Bortezomib also increased RhoA-GTP activity and phosphorylation of myosin light chain (MLC) kinase, which is downstream of RhoA (Figure 4, A and B).

RhoA-dependent signaling has been linked to the production of proplatelets (17, 18). Therefore, we treated human megakaryocytes with Y27632, a selective inhibitor of the Rho-associated protein kinase p160ROCK, or with C3 transferase, a direct RhoA inhibitor. Y27632 and C3 transferase rescued proplatelet formation in bortezomib-treated cells (Figure 4C and Supplemental Figure 7). This response was likely due to inhibition of downstream RhoA effectors, because Y27632 decreased phosphorylation of MLC kinase in the presence of bortezomib (Figure 4B). In agreement with the rescue of proplatelet formation observed in bortezomib-treated human megakaryocytes, mouse megakaryocytes treated with bortezomib plus Y27632 or with bortezomib plus fasudil, a more clinically relevant p160ROCK inhibitor, formed proplatelets (Figure 4D). These results in mouse megakaryocytes were similar to a recent report by Murai et al. (19).

Genetic deletion of the proteasome results in severe thrombocytopenia and death. To further dissect the role of the proteasome in thrombopoiesis, we focused on protease (prosome, macropain) 26S subunit, ATPase 1 (*Psmc1*; gene ID 19179) in mouse megakaryocytes and platelets. *Psmc1* is an essential subunit of the 19S regulatory particle that is critical for ubiquitin-mediated protein degradation by the 26S proteasome complex (20–22). It is conserved at the protein level in human and mouse megakaryocytes (Supplemental Figure 8). mRNA for *Psmc1* was also expressed in both species, although human megakaryocytes had lower levels of the transcript compared with mouse megakaryocytes (Supplemental Table 1).

Psmc1$^{fl/fl}$ mice were crossed with platelet factor 4 *Cre* recombinase (*Pf4-Cre*) mice to disrupt proteasome activity in megakaryocytes and platelets. *Psmc1*$^{fl/fl}$ *Pf4-Cre* mice had significantly reduced protein for PSMC1 in megakaryocytes, but not other tissues (Supplemental Figure 9). Ubiquinated proteins also accumulated in megakaryocytes from *Psmc1*$^{fl/fl}$ *Pf4-Cre* mice (Supplemental Figure 10).

Despite a marked reduction in PSMC1 protein, the number of megakaryocytes from *Psmc1*$^{fl/fl}$ *Pf4-Cre* mice in bone marrow or spleen was not reduced compared with *Psmc1*$^{fl/wt}$ mice (Supplemental Figure 11). Unlike their littermate controls, however, *Psmc1*$^{fl/fl}$ *Pf4-Cre* mice had severe thrombocytopenia at postnatal day 1 (P1), and the majority of *Psmc1*$^{fl/fl}$ *Pf4-Cre* mice died before weaning (Figure 5, A and B). The reduction in platelet counts was more severe than in *c-Mpl* knockout pups at the same age (Supplemental Figure 12). In addition to reduced numbers of platelets, *Psmc1*$^{fl/fl}$ *Pf4-Cre* mice had lower hematocrits than *Psmc1*$^{fl/wt}$ mice, and bleeding was seen in the abdomen and limbs (Figure 5, C and D). Pathological signs of hemorrhage were also present in the bladder and testes of all animals and occasionally observed in the brain, lymph nodes, and intestines (Figure 5E and data not shown).

Ultrastructure examination of megakaryocytes from *Psmc1*$^{fl/fl}$ *Pf4-Cre* mice revealed less cytoplasm compared with megakaryocytes from *Psmc1*$^{fl/wt}$ mice (Figure 6A). In addition, *Psmc1*$^{fl/fl}$ *Pf4-Cre* megakaryocytes lacked demarcation membranes, which were readily visible in *Psmc1*$^{fl/wt}$ megakaryocytes (Figure 6A). Similar to mouse megakaryocytes treated with bortezomib (Figure 2A), megakaryocytes from *Psmc1*$^{fl/fl}$ *Pf4-Cre* mice failed to produce proplatelets (Figure 6B).

Inhibition of RhoA-dependent signaling prevents thrombocytopenia induced by genetic disruption of proteasome activity. As predicted from the pharmacological data, megakaryocytes from *Psmc1*$^{fl/fl}$ *Pf4-Cre* mice expressed higher levels of total RhoA protein and RhoA-GTP

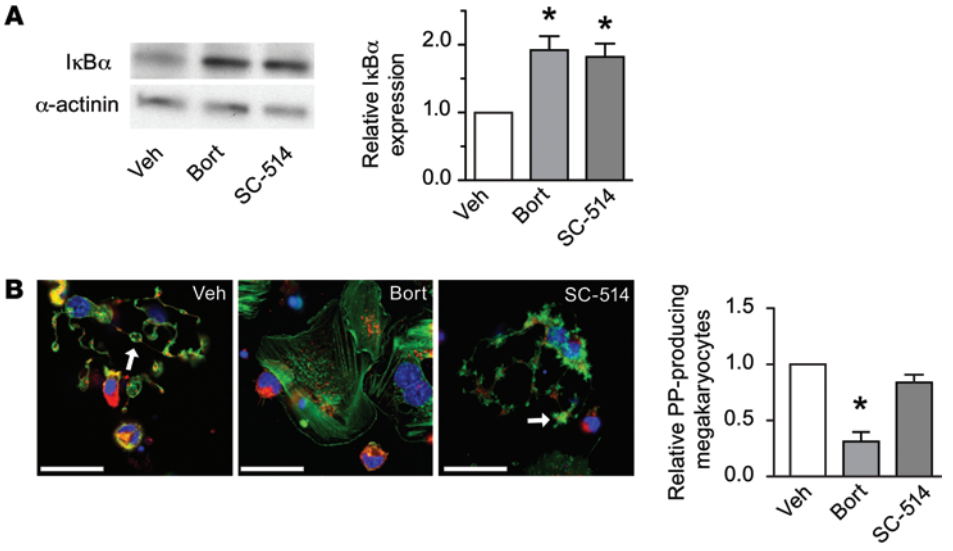

Figure 3. Proteasome-dependent formation of proplatelets in human megakaryocytes occurs independently of NF-κB. (**A**) Human megakaryocytes were treated with vehicle, bortezomib, or the NF-κB inhibitor SC-514. Shown are a representative Western blot for IκBα as well as IκBα expression levels, as measured by densitometry, relative to vehicle control. Data are mean ± SEM (n = 3). (**B**) Morphology of megakaryocytes treated with vehicle, bortezomib, or SC-514. Megakaryocytes were stained with WGA (red), phalloidin (green), and DAPI (blue). Arrows denote proplatelets. Images are representative of 3 independent experiments. Also shown is the number of proplatelet-producing megakaryocytes relative to vehicle control. Data are mean ± SEM of 3 independent experiments. Scale bars: 25 μm. *$P < 0.05$ vs. vehicle.

(Figure 7A). Fasudil also rescued proplatelet formation in bone marrow–derived megakaryocytes from *Psmc1*$^{fl/fl}$ *Pf4-Cre* mice (Figure 7B).

Next we generated inducible conditional knockouts by crossing *Psmc1*$^{fl/fl}$ mice with platelet-derived growth factor–*Cre* estrogen receptor (*Pdgf-Cre-ER*) mice, which allowed for time-restricted deletion of *Psmc1* in megakaryocytes and platelets after administration of the competitive estrogen receptor ligand tamoxifen. Although *Pdgf* is expressed by other cells besides megakaryocytes, *Pdgf-Cre-ER* mice were used because *Pf4-Cre-ER* mouse lines are not currently available. Like *Psmc1*$^{fl/fl}$ *Pf4-Cre* mice (Figure 5, A and B), administration of tamoxifen to *Psmc1*$^{fl/fl}$ *Pdgf-Cre-ER* mice at P1 resulted in thrombocytopenia and early postnatal mortality (Supplemental Figure 13, A and B). When tamoxifen was administered to adult *Psmc1*$^{fl/fl}$ *Pdgf-Cre-ER* mice, platelet counts were reduced by approximately 50% after 6 days compared with *Psmc1*$^{fl/wt}$ mice (Figure 8A). In the presence of fasudil, however, tamoxifen did not significantly decrease platelet counts in *Psmc1*$^{fl/fl}$ *Pdgf-Cre-ER* mice (Figure 8A). Consistent with these rescue experiments, staining of megakaryocytes in crude bone marrow showed that the in vivo fasudil treatment rescued proplatelet formation (Figure 8B). These results are consistent with our in vitro findings that fasudil maintained proplatelet formation in bortezomib-treated megakaryocytes (Figure 4D).

Discussion

In this study, we found that pharmacologic or genetic disruption of proteasome activity in megakaryocytes inhibits proplatelet formation. Pharmacologic inhibition was reversible in megakaryocytes treated in vitro with bortezomib, and thrombocytopenia was transient when bortezomib was administered as a bolus in vivo. When inhibition of proteasome activity was sustained, as was the case with genetic deletion of *Psmc1* in megakaryocytes and platelets, megakaryocytes did not form proplatelets, and *Psmc1*$^{fl/fl}$ *Pf4-Cre* mice had severe thrombocytopenia. Mice with genetic ablation of *Psmc1* in megakaryocytes and platelets also died shortly after birth. Taken together, these data provide compelling evidence that the proteasome is critically involved in thrombopoiesis. The data also offer a strong explanation as to why multiple myeloma patients require cyclic treatment regimes of bortezomib in order to tolerate the drug (3, 12).

Our findings provide definitive proof that the megakaryocyte proteasome is required for the final stages of platelet production. Evidence for this is 2-fold: first, pharmacologic inhibition of proteasome activity in late-stage human or mouse megakaryocytes significantly blunted proplatelet formation; and second, platelet production was significantly reduced in *Psmc1*$^{fl/fl}$ *Pf4-Cre* mice, in which genetic deletion of *Psmc1* does not occur until megakaryocytes express platelet factor 4, which activates the *Cre* recombinase (23). In addition to regulating thrombopoiesis, others have shown that the proteasome is important for the proliferation of megakaryocyte precursors (24) and the degradation of cyclin B and pro–integrin α_{IIb} in megakaryocytes (5, 25).

Like their parent megakaryocytes, anucleate platelets also possess proteasome activity (4, 10), and several groups have demonstrated that pharmacologic inhibition of the proteasome regulates platelet function (8–11, 26). Under the conditions of our experiments, bortezomib did not affect indices of platelet activation in mouse or human platelets that included activation of integrin $\alpha_{IIb}\beta_3$ and translocation of P-selectin to the surface of platelets. However, similar to Gupta and coworkers (8), we observed that bortezomib reduced the aggregation of human platelets when low concentrations of thrombin were used as the agonist (Supplemental Figure 14). Although more work is needed, results generated by multiple independent groups strongly indicate that protein degradation systems regulate platelet function (6).

Other groups have shown that pharmacologic inhibition regulates the function of platelets ex vivo (8–11, 26), but bortezomib did not accelerate the clearance of labeled platelets under the conditions of our present studies. Our results contrasted those of Nayak and colleagues (7), who showed that pharmacologic inhibition of the proteasome reduced the half-life of platelets in mice. One potential explanation for these discordant findings is that the bolus dose of bortezomib used in our studies only produced a mild thrombocytopenia and did not completely abolish platelet proteasome activity (Figure 1A). Although Nayak's group did not measure cellular proteasome activity (7), it is possible that they achieved more efficient pharmacologic inhibition of the proteasome in platelets and other vascular cells. Different routes of drug administra-

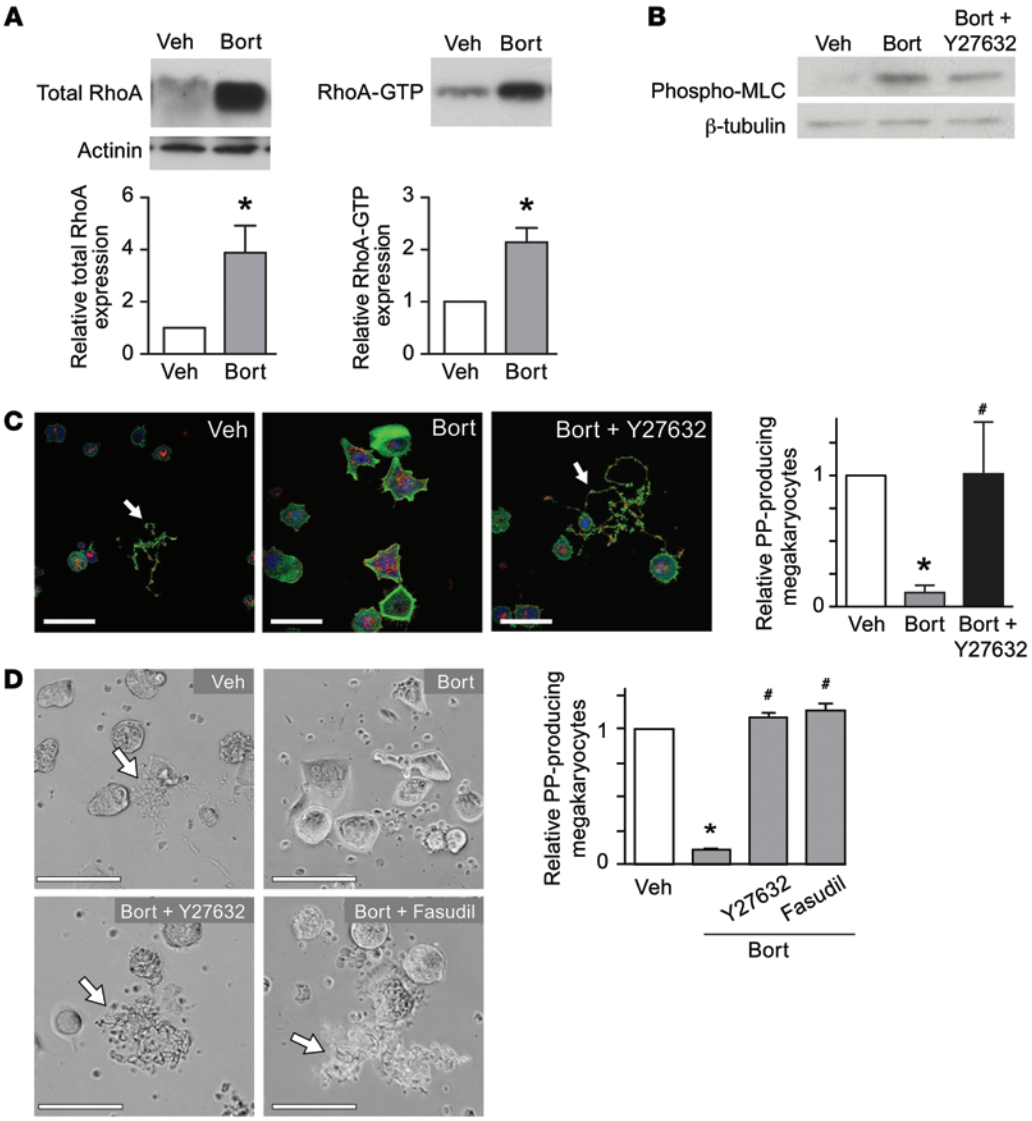

Figure 4. The proteasome regulates proplatelet formation through the RhoA signaling pathway. (**A**) Human megakaryocytes were treated with vehicle or bortezomib, and total RhoA and GTP-bound RhoA were measured. Shown are representative Western blots and expression of RhoA or RhoA-GTP, as measured by densitometry, relative to vehicle control. Data are mean ± SEM of 4 independent experiments. (**B** and **C**) Human megakaryocytes were treated with vehicle, bortezomib, or bortezomib plus Y27632. (**B**) Western blot for phospho-MLC. (**C**) Representative confocal images of human megakaryocytes stained with WGA (red) and phalloidin (green). Arrows denote proplatelets. Scale bar: 50 μm. Also shown is the number of proplatelet-producing megakaryocytes relative to vehicle control. Data are mean ± SEM of 3 independent experiments. (**D**) Representative transmission images of mouse bone marrow–derived megakaryocytes treated with vehicle, bortezomib, bortezomib plus Y27632, or bortezomib plus fasudil. Scale bar: 100 μm. Also shown is the number of proplatelet-producing megakaryocytes relative to vehicle control. Data are mean ± SEM of 3 independent experiments. $^{*}P < 0.05$ vs. vehicle; $^{\#}P < 0.05$ vs. bortezomib alone.

tion and types/concentrations of proteasome inhibitors between the studies may also explain the divergent results. Further studies are needed to resolve the in vivo pharmacology of proteasome inhibition and its relation to thrombocytopenia. However, our present studies clearly showed that platelet counts rebounded at a slower pace in mice subjected to platelet depletion in the presence of bortezomib. These data, in combination with the severe thrombocytopenia we observed in *Psmc1*$^{fl/fl}$ *Pf4-Cre* mice, demonstrated that the proteasome directly modulates platelet production.

We found that thrombocytopenia was more severe in *Psmc1*$^{fl/fl}$ *Pf4-Cre* mice compared with *c-Mpl* knockout mice (Supplemental Figure 12), which have normal life expectancies (27). Consistent with a marked reduction in platelet counts, *Psmc1*$^{fl/fl}$ *Pf4-Cre* mice had low hematocrits and hemorrhaging in the abdominal region. Occasional hemorrhaging was also observed in the brain, lymph nodes, and intestines. This suggests that severe thrombocytopenia is the primary driver of postnatal death in *Psmc1*$^{fl/fl}$ *Pf4-Cre* mice. Hemorrhaging in *Psmc1*$^{fl/fl}$ *Pf4-Cre* mice may occur because platelet numbers are simply too low to prevent bleeding. Alternatively, insufficient platelet counts in *Psmc1*$^{fl/fl}$ *Pf4-Cre* mice may result in abnormal vascular development or blood/lymphatic vessel separation, which could lead to excessive bleeding (28). In this regard, several groups have shown that platelet C-type lectin-like receptor 2 (CLEC-2) receptors regulate lymphatic vascular development, and, like *Psmc1*$^{fl/fl}$ *Pf4-Cre* mice (29–33), platelet-specific knockout of *CLEC-2* results in postnatal lethality (32). It should also be noted that a very low threshold of platelet function sufficiently maintains vascular function (27, 33, 34), raising the possibility that *Psmc1*$^{fl/fl}$ *Pf4-Cre* mice produce dysfunctional platelets that are incapable of maintaining vascular integrity. Indeed, recent studies have demonstrated that immune-type receptors in platelets are critical for the prevention of inflammation-induced hemorrhage (35). Thus, it is entirely possible that in addition to being reduced in number, platelets from *Psmc1*$^{fl/fl}$ *Pf4-Cre* mice express an abnormal repertoire of proteins resulting in platelet dysfunction.

Studies in megakaryocytes revealed that genetic or pharmacologic interruption of proteasome activity led to accumulation of IκBα and RhoA. Although both proteins were upregulated, we found that the final stages of proplatelet formation required RhoA signaling rather than inhibition of NF-κB, as previously suggested (12). The inability to sprout proplatelets resembled studies in neu-

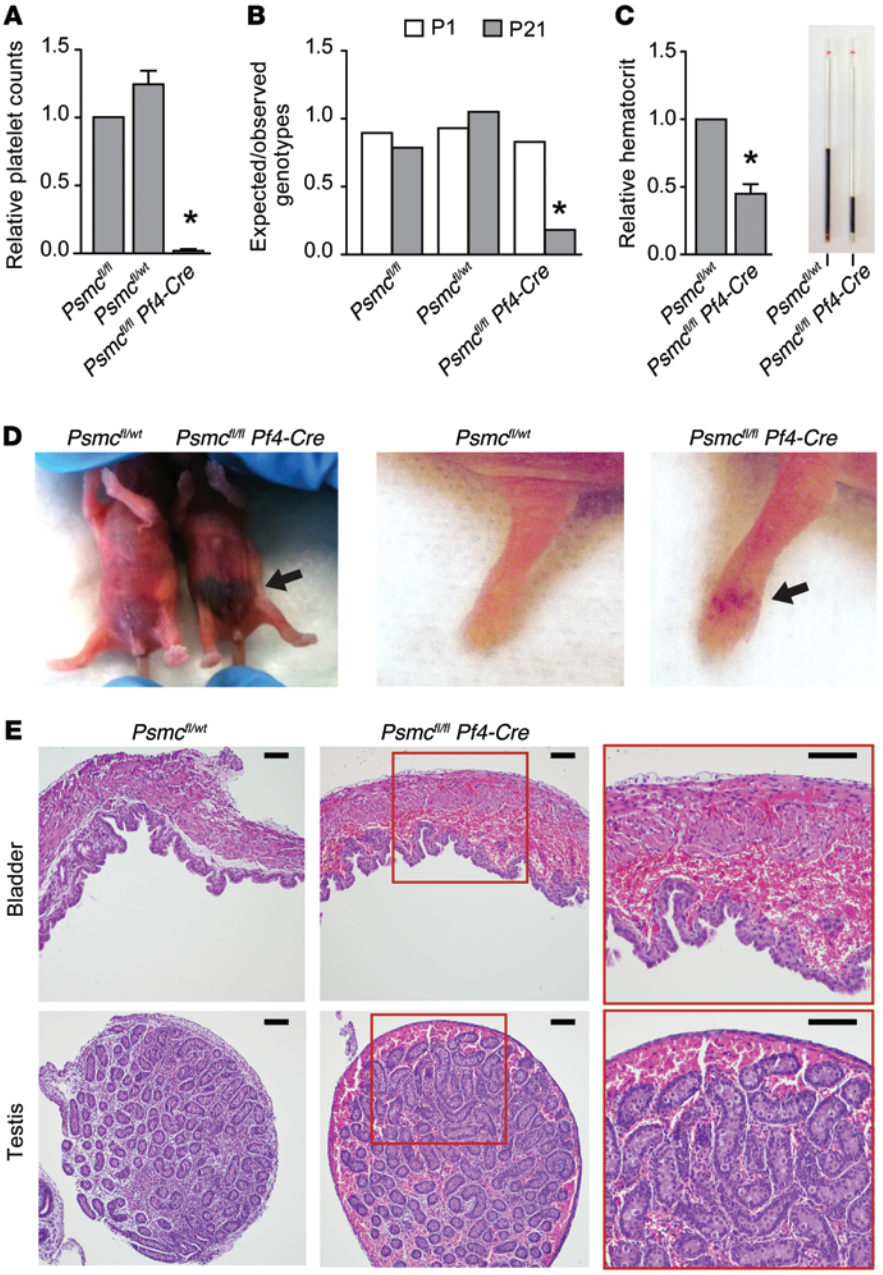

Figure 5. Genetic ablation of proteasome activity in megakaryocytes causes severe thrombocytopenia and postnatal death. (**A**) Platelet counts at P1 in *Psmc1*$^{fl/fl}$ *Pf4-Cre* and *Psmc1*$^{fl/wt}$ mice, expressed relative to *Psmc1*$^{fl/fl}$ mice. Bars show mean ± SEM of 6 independent experiments. *$P < 0.05$ vs. *Psmc1*$^{fl/fl}$. (**B**) Mortality rates in *Psmc1*$^{fl/fl}$, *Psmc1*$^{fl/wt}$, and *Psmc1*$^{fl/fl}$ *Pf4-Cre* mice at P1 and P21. Shown are ratios of expected versus observed genotypes, determined by χ^2 analysis, at P1 and P21 ($n = 88$). *$P < 0.05$ vs. P1, determined by χ^2 distribution table. (**C**) Hematocrits in *Psmc1*$^{fl/fl}$ *Pf4-Cre* relative to *Psmc1*$^{fl/wt}$ mice at P1. Data are mean ± SEM of 6 independent experiments. *$P < 0.05$ vs. *Psmc1*$^{fl/wt}$. (**D**) Left: Images of *Psmc1*$^{fl/wt}$ and *Psmc1*$^{fl/fl}$ *Pf4-Cre* mice at P1. Evidence of bleeding was observed in the abdominal region (arrow). Middle and right: Limbs of *Psmc1*$^{fl/wt}$ and *Psmc1*$^{fl/fl}$ *Pf4-Cre* mice. Hemorrhaging was observed in the limb of the *Psmc1*$^{fl/fl}$ *Pf4-Cre* mouse (arrow). (**E**) Whereas P1 histological sections of *Psmc1*$^{fl/wt}$ mice demonstrated normal histology, bleeding was observed in the bladder and testis of a *Psmc1*$^{fl/fl}$ *Pf4-Cre* mouse. Boxed regions are shown at higher magnification at right. Scale bars: 100 μm.

rons, in which acute inhibition of the proteasome blocks activity-dependent growth of new dendritic spines. It is not known what proteins are degraded by the proteasome in order to stimulate new spine growth; however, inactivation of RhoA leads to neurite outgrowth (36, 37). This suggests that, similar to megakaryocyte proplatelet formation, the proteasome may control neuronal outgrowth by degrading RhoA. Moreover, RhoA signaling has been shown to maintain normal megakaryocyte development, which is critical for platelet production (18).

Malfunction of the proteasome in human diseases may lead to aberrant platelet production or abnormal platelet generation. Disruption of proteasome activity could occur at multiple checkpoints, since human megakaryocytes expressed the full repertoire of proteasome components at the mRNA level (Supplemental Table 1). Identifying the complete portfolio of target proteins degraded by the proteasome in megakaryocytes will shed additional light on the mechanisms that control thrombopoiesis and the phenotype of platelets as they enter the circulation. Understanding the functions of the proteasome in platelets, which is active and capable of degrading proteins (7–9), also requires further investigation. From an immediate perspective, our present findings demonstrated that bortezomib directly inhibits proteasome activity in megakaryocytes and thereby decreases platelet production. Our findings also established fasudil as a potential treatment for preventing and/or reversing bortezomib-induced thrombocytopenia in multiple myeloma patients. Additionally, inhibitors of the RhoA signaling pathway may have efficacy in the treatment of other thrombocytopenic disorders caused by abnormal platelet production, especially if the disease is driven by proteasome-dependent mechanisms.

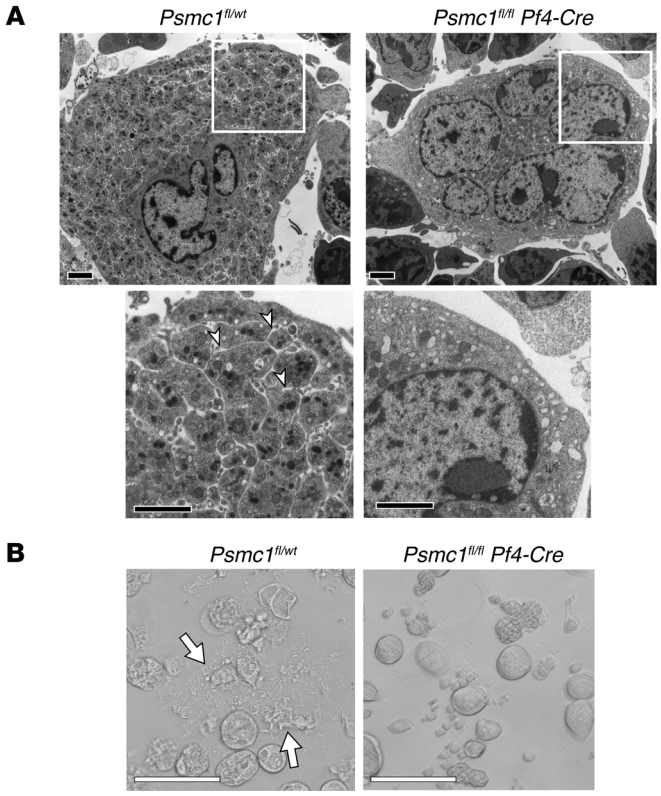

Figure 6. Platelet territories and proplatelets fail to form in PSMC1-deficient megakaryocytes. (**A**) Whereas *Psmc1*$^{fl/wt}$ mouse megakaryocytes showed a large cytoplasmic region compared with the nucleus, those from a *Psmc1*$^{fl/fl}$ *Pf4-Cre* mouse had less cytoplasm compared with the multilobed nucleus. Boxed regions are shown at higher magnification below, in which the demarcation membrane exhibited in the *Psmc1*$^{fl/wt}$ megakaryocytes (arrowheads) was not observed in the *Psmc1*$^{fl/fl}$ *Pf4-Cre* megakaryocyte. (**B**) Transmission images of megakaryocytes derived from *Psmc1*$^{fl/wt}$ and *Psmc1*$^{fl/fl}$ *Pf4-Cre* mice at P1. Proplatelet formation (arrows) was absent in *Psmc1*$^{fl/fl}$ *Pf4-Cre* mice. Scale bars: 2 μm (**A**); 100 μm (**B**).

Methods

Differentiation of human and mouse megakaryocytes

Cord blood from normal full-term deliveries was obtained, and CD34$^+$ hematopoietic progenitors were isolated and differentiated into megakaryocytes as previously described (38, 39). Mature megakaryocytes were placed on immobilized human fibrinogen–coated surfaces in the presence of specific inhibitors or their vehicle, and the number of megakaryocytes that possessed proplatelets was counted by an independent blinded observer. On average, 12% ± 3% of vehicle-treated megakaryocytes had proplatelet extensions.

Mouse megakaryocytes were isolated from fetal liver as previously described (40). Mouse bone marrow–derived megakaryocytes were obtained using modifications of a published report (41). For the bone marrow megakaryocytes, C57BL/6 mice (8–10 weeks of age) were euthanized, and cells were obtained from the bone marrow of femur and tibia by flushing the bone marrow. Cells were homogenized by pipetting followed by passage through a 100-μm filter. The cell population was resuspended in 10% fetal bovine serum–supplemented DMEM with 2 mM L-glutamine, penicillin/streptomycin, and fibroblast condition media containing thrombopoietin. The cells were cultured for 5 days (37°C and 5% CO_2), and mature megakaryocytes were layered over a bovine serum albumin (BSA) gradient as described previously (42). Fetal liver and bone marrow–derived megakaryocytes were subsequently resuspended in culture media as described above, then placed on immobilized BSA or fibrinogen in the presence or absence of inhibitors, and megakaryocytes with proplatelets were counted. On average, 34% ± 1% of vehicle-treated fetal liver–derived megakaryocytes produced proplatelets. Proplatelet formation in vehicle-treated bone marrow–derived megakaryocytes was 50% ± 1%.

Inhibitors used in these in vitro studies (all diluted in DMSO) included bortezomib (100 nM; Selleck Chem), Y27632 (10 μM; Sigma-Aldrich), fasudil (10 μM; Selleck Chem), C3 transferase (10 μM; Cytoskeleton Inc.), SC-514 (0.5 μM; Calbiochem), MG132 (10 μM; Sigma-Aldrich), and lactacystin (10 μM; Sigma-Aldrich). Inhibitors were administered at different times, as indicated in the figure legends.

Next-generation RNA-Seq

Fetal liver–derived megakaryocytes for RNA-Seq were provided by J. Thon (Harvard Medical School, Boston, Massachusetts, USA). RNA from human CD34-differentiated or fetal liver–derived proplatelet-producing megakaryocytes was isolated and prepped for deep sequencing as previously described (43–45). In brief, RNA was prepared for sequencing according to Illumina's (DNA vision) TruSeq kit V2 for poly-A RNA. Libraries were sequenced 36 (human) and 50 (mouse) base pairs on an Illumina sequencer. Reads were aligned using Novoalign (Novocraft Technologies) software followed by processing, including RPKM assignment, using the USeq analysis package (46). The processed RNA-Seq data and aligned reads were deposited in GEO (accession no. GSE58202; ref. 47).

Protein expression analyses and assessment of RhoA activity

Cell lysates were placed in laemmli buffer, proteins were separated by SDS-page, and IκBα and phospho-MLC (Cell Signaling) were analyzed by Western blotting. To measure RhoA activity, platelets were placed in Mg^{2+} lysis buffer supplemented with protease (Roche Applied Science) and phosphatase inhibitors (Sigma-Aldrich). A small portion of the lysate was retained as total cell lysate, and the rest was incubated with the assay reagent. GTP-bound forms were eluted from the assay reagent using Laemmli sample buffer. Total RhoA and RhoA-GTP bound protein were analyzed by Western blotting using a pulldown kit (Millipore).

Mouse in vivo studies

In vivo measurements of platelets. In Figure 1A, platelet counts were determined at various time points with a Hemavet 950 (Drew Scientific). For platelet clearance, C57BL/6 mice were injected intravenously (i.v.) on day 0 with anti-GPIBβ Dylight 488 (0.1 μg/g body weight; Emfret Analytics) and intraperitoneally (i.p.) with bortezomib (2 mg/kg body weight) or its vehicle (10% DMSO in 0.9% saline). Blood samples (30 μl) were taken daily, diluted in Hanks balanced salt solution, and stained with a phycoerythrin-conjugated anti-mouse CD41 antibody (BD Biosciences), and clearance of Dylight 488–positive platelets was measured as previously described (48).

For estimation of platelet production, C57BL/6 mice were injected i.v. on day 0 with anti-GPIBα antibodies (3 μg/g body weight; Emfret Analytics) to deplete circulating platelets. On day 1,

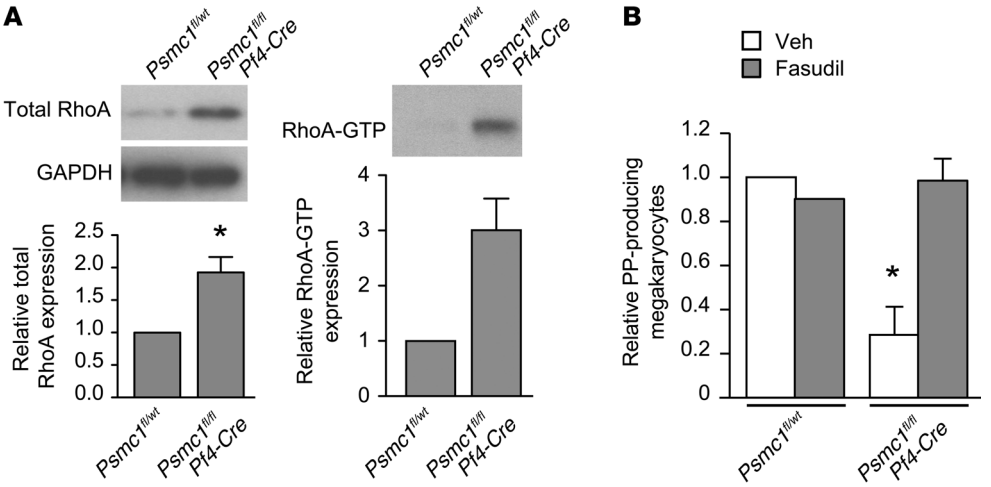

Figure 7. Genetic deletion of *Psmc1* in megakaryocytes is associated with increased RhoA protein and activity. (**A**) Representative Western blot of total RhoA and RhoA-GTP in megakaryocytes derived from *Psmc1*$^{fl/wt}$ and *Psmc1*$^{fl/fl}$ *Pf4-Cre* mice at P1. Also shown is densitometry quantification relative to *Psmc1*$^{fl/wt}$ control; for RhoA-GTP, megakaryocytes were isolated from 10 P1 mice, lysed, and then the lysates were pooled together for each pulldown experiment (see Methods). Data are mean ± SEM of 3 (total RhoA) and 2 (RhoA-GTP) experiments. *$P < 0.05$ vs. *Psmc1*$^{fl/wt}$. (**B**) Bone marrow–derived megakaryocytes from *Psmc1*$^{fl/wt}$ and *Psmc1*$^{fl/fl}$ *Pf4-Cre* mice were treated with vehicle or fasudil, and the number of proplatelet-producing megakaryocytes was quantified and expressed relative to *Psmc1*$^{fl/wt}$ controls. Data are mean ± SEM of 3 independent experiments. *$P < 0.05$ vs. vehicle-treated *Psmc1*$^{fl/wt}$.

platelet counts were assessed to confirm depletion; shortly after, mice were treated i.p. with bortezomib or its vehicle as above. Blood samples (2 μl) were taken daily for the remainder of the experiment, and platelet counts were measured by flow cytometry as previously described (13).

Knockout of the proteasome in mouse megakaryocytes and platelets. Megakaryocyte and platelet ablation of proteasome activity was achieved by crossing *Psmc1*$^{fl/fl}$ mice (provided by J. Mayer, Baylor College of Medicine, Houston, Texas, USA) with *Pf4-Cre* or *Pdgf-Cre-ER* mice (Jackson Labs), generating *Psmc1*$^{fl/wt}$ and *Psmc1*$^{fl/fl}$ *Pf4-Cre* mice or *Psmc1*$^{fl/wt}$ and *Psmc1*$^{fl/fl}$ *Pdgf-Cre-ER* mice. *Psmc1*$^{fl/fl}$ mice were also used as controls in select studies. Knockdown was confirmed in megakaryocytes using an antibody against PSMC1 (Novus Biologicals), and platelet counts were assessed as recently described (49). Tamoxifen (0.25 mg/kg) was administered i.p. to *Psmc1*$^{fl/fl}$ *Pdgf-Cre-ER* pups on P1, and then mortality was monitored from P2 to P21. For studies in adult *Psmc1*$^{fl/fl}$ *Pdgf-Cre-ER* mice, tamoxifen was administered 8 weeks after birth. In these mice, fasudil (5 mg/kg) was injected i.p. to *Psmc1*$^{fl/fl}$ *Pdgf-Cre-ER* mice 4 and 48 hours after tamoxifen administration, and blood was retrieved from tail veins on day 6 after tamoxifen to determine circulating platelet counts. In a subset of mice ($n = 2$ per treatment group), ex vivo assessment of proplatelet formation was performed. For these studies, mice were euthanized via CO_2 asphyxiation followed by cervical dislocation. Femurs were isolated, and bone marrow cords were flushed with HEPES-tyrodes buffer with 100 U/ml penicillin/streptomycin. Crude bone marrow cords were sliced into multiple sections, and buffer was replaced with HEPES-tyrodes buffer with 5% mouse serum and 100 U/ml penicillin/streptomycin. Bone marrow sections were then incubated at 37°C for 2 hours and stained with

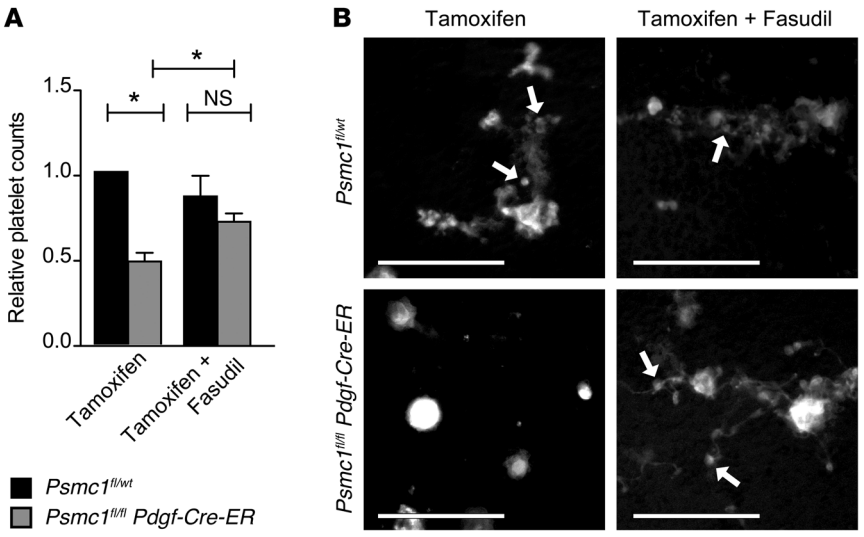

Figure 8. Inhibition of RhoA signaling rescues platelet counts in adult mice in which proteasome activity is conditionally deleted. (**A**) Tamoxifen was administered to adult *Psmc1*$^{fl/wt}$ and *Psmc1*$^{fl/fl}$ *Pdgf-Cre-ER* mice, followed by treatment with fasudil or saline control (4 and 48 hours after tamoxifen). Shown are platelet counts at day 6 after tamoxifen administration relative to *Psmc1*$^{fl/wt}$ controls treated with tamoxifen alone. Data are mean ± SEM of 9 experiments performed on independent mice. *$P < 0.05$ as indicated. No significant difference was observed between groups treated with tamoxifen plus fasudil. (**B**) Representative images of Dylight 488–positive megakaryocytes present in crude bone marrow isolated from *Psmc1*$^{fl/wt}$ and *Psmc1*$^{fl/fl}$ *Pdgf-Cre-ER* mice immediately after euthanasia. Bone marrow for these studies was isolated from a subset of the mice in **A** ($n = 2$ per treatment group). Scale bars: 100 μm.

anti-GPIBβ Dylight 488. Megakaryocytes were imaged on a Nikon Eclipse TS100 fluorescence microscope and quantified by counting 10 fields (×20) per well.

Measurement of blood hematocrit

Hematocrit was measured in *Psmc1*$^{fl/wt}$ and *Psmc1*$^{fl/fl}$ *Pf4-Cre* mice at P3. After anesthesia (ketamine-xylazine; 0.2 mg/g body weight), blood was acquired via the retro-orbital venous plexus. Blood was collected into heparinized capillary tubes and spun at 50,000 *g* for 10 minutes to obtain a hematocrit for each mouse.

Histopathology

Organs from P1 mice were collected and fixed in neutral buffered formalin. Tissues were embedded in paraffin, sectioned at 10 μm, and stained with hematoxylin and eosin (H&E). Slides were then assessed by a hematopathologist.

Electron microscopy

Femurs from mice were collected, and bone marrow was flushed into glutaraldehyde 2.5% in PBS. Fixed samples were kept at 4°C, shipped to the Hospital for Sick Children in Toronto, and further processed and imaged as previously described (50).

Statistics

For multiple-group comparisons, data were subjected to 1-way analysis of variance (ANOVA), and Tukey's post-hoc test was used to assess statistical significance among groups. 2-way ANOVA with Newman-Keuls post-hoc test was used to assess statistical significance for the data in Figure 8B. 2-tailed Student's *t* test was used when comparisons were made between 2 groups. Differences in mortality were assessed by χ^2 test, and observed outcomes were graphed relative to calculated expected outcomes (Figure 5B and Supplemental Figure 13B). When possible, quantifications were done by a blinded observer. *P* values less than 0.05 were considered statistically significant.

All data graphed relative to controls (Figures 2–5, 7, and 8 and Supplemental Figures 4, 7, 10, and 13) were generated by comparing the average of the data set in each treated group with that of the control group (as the denominator).

Study approval

The human studies were approved by the University of Utah's Institutional Review Board (IRB no. 392). All participating subjects provided informed consent. Cord blood from normal full-term deliveries was obtained after informed consent by the mothers (IRB no. 11919). The mouse studies were approved by the University of Utah's Institutional Animal Care and Review Board (IACUC nos. 12-10002 and 12-11017) or by the Children's Hospital in Boston (IACUC no. A3431-01).

Further information can be found in the supplemental material and citations therein (51, 52).

Acknowledgments

We thank Diana Lim for preparation of the figures, critical comments, and consultation regarding responsible and effective display of the images. We also thank Guy Zimmerman for helpful discussions regarding the roles of the proteasome in platelets and megakaryocytes. This work was funded by NIH grants HL066277 and HL112311 (to A.S. Weyrich), HL112311, HL084516, and AR064788 (to D.Y. Li), GM103806 (to J.W. Rowley), and HL68130 (to J.E. Italiano Jr.); by the American Heart Association (13POST13930019 to K.R. Machlus; 11POST7290019 to R.A. Campbell; 0625098Y and 09BG1A2250381 to H. Schwertz); and by the Canadian Institutes of Health Research (MOP-259952 to W.H.A. Kahr). In addition, H. Schwertz was funded by a Lichtenberg-Professorship from the Volkswagen Foundation.

Address correspondence to: Dean Li or Andrew S. Weyrich, Eccles Institute of Human Genetics, 15 North 2030 East, Bldg. 533, Rm. 4150, Salt Lake City, Utah 84112, USA. Phone: 801.585.0950; E-mail: dean.li@u2m2.utah.edu (D. Li), andy.weyrich@u2m2.utah.edu (A.S. Weyrich).

1. Adams J, et al. Proteasome inhibitors: a novel class of potent and effective antitumor agents. *Cancer Res*. 1999;59(11):2615–2622.
2. Richardson PG, et al. A phase 2 study of bortezomib in relapsed, refractory myeloma. *N Engl J Med*. 2003;348(26):2609–2617.
3. Field-Smith A, Morgan GJ, Davies FE. Bortezomib (Velcadetrade mark) in the treatment of multiple myeloma. *Ther Clin Risk Manag*. 2006;2(3):271–279.
4. Ostrowska H, Ostrowska JK, Worowski K, Radziwon P. Human platelet 20S proteasome: inhibition of its chymotrypsin-like activity identification of the proteasome activator PA28. A preliminary report. *Platelets*. 2003;14(3):151–157.
5. Mitchell WB, Li J, French DL, Coller BS. αIIbβ3 biogenesis is controlled by engagement of αIIb in the calnexin cycle via the N15-linked glycan. *Blood*. 2006;107(7):2713–2719.
6. Kraemer BF, Weyrich AS, Lindemann S. Protein degradation systems in platelets. *Thromb Haemost*. 2013;110(5):920–924.
7. Nayak MK, Kulkarni PP, Dash D. Regulatory role of proteasome in determination of platelet life span. *J Biol Chem*. 2013;288(10):6826–6834.
8. Gupta N, Li W, Willard B, Silverstein RL, McIntyre TM. Proteasome proteolysis supports stimulated platelet function and thrombosis. *Arterioscler Thromb Vasc Biol*. 2014;34(1):160–168.
9. Kumari S, Dash D. Regulation of β-catenin stabilization in human platelets. *Biochimie*. 2013;95(6):1252–1257.
10. Nayak MK, Kumar K, Dash D. Regulation of proteasome activity in activated human platelets. *Cell Calcium*. 2011;49(4):226–232.
11. Avcu F, Ural AU, Cetin T, Nevruz O. Effects of bortezomib on platelet aggregation and ATP release in human platelets, in vitro. *Thromb Res*. 2008;121(4):567–571.
12. Lonial S, et al. Risk factors and kinetics of thrombocytopenia associated with bortezomib for relapsed, refractory multiple myeloma. *Blood*. 2005;106(12):3777–3784.
13. Mason KD, et al. Programmed anuclear cell death delimits platelet life span. *Cell*. 2007;128(6):1173–1186.
14. McConkey DJ. Bortezomib paradigm shift in myeloma. *Blood*. 2009;114(5):931–932.
15. Spinelli SL, et al. Platelets and megakaryocytes contain functional nuclear factor-kappaB. *Arterioscler Thromb Vasc Biol*. 2010;30(3):591–598.
16. Whitehead KJ, et al. The cerebral cavernous malformation signaling pathway promotes vascular integrity via Rho GTPases. *Nat Med*. 2009;15(2):177–184.
17. Gobbi G, et al. Proplatelet generation in the mouse requires PKCepsilon-dependent RhoA inhibition. *Blood*. 2013;122(7):1305–1311.
18. Suzuki A, et al. RhoA is essential for maintaining normal megakaryocyte ploidy and platelet generation. *PLoS One*. 2013;8(7):e69315.
19. Murai K, et al. Bortezomib induces thrombocytopenia by the inhibition of proplatelet formation of megakaryocytes [published online ahead of print April 21, 2014]. *Eur J Haematol*. doi:10.1111/ejh.12342.
20. Rubin DM, Glickman MH, Larsen CN, Dhruvakumar S, Finley D. Active site mutants in the six regulatory particle ATPases reveal multiple roles for ATP in the proteasome. *EMBO J*. 1998;17(17):4909–4919.
21. Kohler A, Cascio P, Leggett DS, Woo KM, Gold-

berg AL, Finley D. The axial channel of the proteasome core particle is gated by the Rpt2 ATPase controls both substrate entry product release. *Mol Cell*. 2001;7(6):1143–1152.
22. Smith DM, Fraga H, Reis C, Kafri G, Goldberg AL. ATP binds to proteasomal ATPases in pairs with distinct functional effects, implying an ordered reaction cycle. *Cell*. 2011;144(4):526–538.
23. Tiedt R, Schomber T, Hao-Shen H, Skoda RC. Pf4-Cre transgenic mice allow the generation of lineage-restricted gene knockouts for studying megakaryocyte platelet function in vivo. *Blood*. 2007;109(4):1503–1506.
24. Galimberti S, et al. PS-341 (Bortezomib) inhibits proliferation induces apoptosis of megakaryoblastic MO7-e cells. *Leuk Res*. 2008;32(1):103–112.
25. Zhang Y, Wang Z, Liu DX, Pagano M, Ravid K. Ubiquitin-dependent degradation of cyclin B is accelerated in polyploid megakaryocytes. *J Biol Chem*. 1998;273(3):1387–1392.
26. Necchi V, et al. Ubiquitin/proteasome-rich particulate cytoplasmic structures (PaCSs) in the platelets and megakaryocytes of ANKRD26-related thrombo-cytopenia. *Thromb Haemost*. 2012;109(2):263–271.
27. Murone M, Carpenter DA, de Sauvage FJ. Hematopoietic deficiencies in c-mpl and TPO knockout mice. *Stem Cells*. 1998;16(1):1–6.
28. Bertozzi CC, Hess PR, Kahn ML. Platelets: covert regulators of lymphatic development. *Arterioscler Thromb Vasc Biol*. 2010;30(12):2368–2371.
29. Benezech C, et al. CLEC-2 is required for development maintenance of lymph nodes. *Blood*. 2014;123(20):3200–3207.
30. Herzog BH, et al. Podoplanin maintains high endothelial venule integrity by interacting with platelet CLEC-2. *Nature*. 2013;502(7469):105–109.
31. Osada M, et al. Platelet activation receptor CLEC-2 regulates blood/lymphatic vessel separation by inhibiting proliferation, migration, tube formation of lymphatic endothelial cells. *J Biol Chem*. 2012;287(26):22241–22252.
32. Finney BA, et al. CLEC-2 and Syk in the megakaryocytic/platelet lineage are essential for development. *Blood*. 2012;119(7):1747–1756.
33. Bertozzi CC, et al. Platelets regulate lymphatic vascular development through CLEC-2-SLP-76 signaling. *Blood*. 2010;116(4):661–670.
34. Levin J, et al. Pathophysiology of thrombocytopenia and anemia in mice lacking transcription factor NF-E2. *Blood*. 1999;94(9):3037–3047.
35. Boulaftali Y, et al. Platelet ITAM signaling is critical for vascular integrity in inflammation. *J Clin Invest*. 2013;123(2):908–916.
36. Hamilton AM, et al. Activity-dependent growth of new dendritic spines is regulated by the proteasome. *Neuron*. 2012;74(6):1023–1030.
37. Jeon CY, et al. Control of neurite outgrowth by RhoA inactivation. *J Neurochem*. 2012;120(5):684–698.
38. Foulks JM, et al. PAF-acetylhydrolase expressed during megakaryocyte differentiation inactivates PAF-like lipids. *Blood*. 2009;113(26):6699–6706.
39. Denis MM, et al. Escaping the nuclear confines: signal-dependent pre-mRNA splicing in anucleate platelets. *Cell*. 2005;122(3):379–391.
40. Thon JN, Italiano JE. Visualization and manipulation of the platelet and megakaryocyte cytoskeleton. *Methods Mol Biol*. 2012;788:109–125.
41. Mazharian A, Watson SP, Severin S. Critical role for ERK1/2 in bone marrow fetal liver-derived primary megakaryocyte differentiation, motility, proplatelet formation. *Exp Hematol*. 2009;37(10):1238–1249.
42. Thon JN, et al. Cytoskeletal mechanics of proplatelet maturation and platelet release. *J Cell Biol*. 2010;191(4):861–874.
43. Cecchetti L, Tolley ND, Michetti N, Bury L, Weyrich AS, Gresele P. Megakaryocytes differentially sort mRNAs for matrix metalloproteinases and their inhibitors into platelets: a mechanism for regulating synthetic events. *Blood*. 2011;118(7):1903–1911.
44. Kahr WH, et al. Mutations in NBEAL2, encoding a BEACH protein, cause gray platelet syndrome. *Nat Genet*. 2011;43(8):738–740.
45. Rowley JW, et al. Genome-wide RNA-seq analysis of human and mouse platelet transcriptomes. *Blood*. 2011;118(14):e101–e111.
46. Nix DA, Courdy SJ, Boucher KM. Empirical methods for controlling false positives and estimating confidence in ChIP-Seq peaks. *BMC Bioinformatics*. 2008;9.
47. Edgar R, Domrachev M, Lash AE. Gene Expression Omnibus: NCBI gene expression and hybridization array data repository. *Nucleic Acids Res*. 2002;30(1):207–210.
48. Josefsson EC, White MJ, Dowling MR, Kile BT. Platelet life span and apoptosis. *Methods Mol Biol*. 2012;788:59–71.
49. Liu ZJ, et al. Expansion of the neonatal platelet mass is achieved via an extension of platelet lifespan. *Blood*. 2014;123(22):3381–3389.
50. Kahr WH, et al. Abnormal megakaryocyte development and platelet function in Nbeal2(–/–) mice. *Blood*. 2013;122(19):3349–3358.
51. Holly SP, et al. Chemoproteomic discovery of AADACL1 as a regulator of human platelet activation. *Chem Biol*. 2013;20(9):1125–1134.
52. Ramskold D, Wang ET, Burge CB, Sandberg R. An abundance of ubiquitously expressed genes revealed by tissue transcriptome sequence data. *PLoS Comput Biol*. 2009;5(12):e1000598.